Analysis of Active Suspension Performance Improvement Based on Introducing Front/Rear LQ Control Coupling

Ivan Cvok[1(✉)] , Joško Deur[1], H. Eric Tseng[2], and Davor Hrovat[3]

[1] University of Zagreb, Zagreb, Croatia
`ivan.cvok@fsb.hr`
[2] Ford Motor Company, Dearborn, MI, USA
[3] University of California, San Diego, CA, USA

Abstract. The paper investigates the potential of improving vehicle ride comfort based on introducing control design coupling between front- and rear-axle active suspensions. The considered linear quadratic regulator (LQR) cost function includes conflicting criteria related to ride comfort, vehicle handling, and suspension stroke. A covariance analysis related to standard deviations of cost function criteria with respect to stochastic road profile input is carried out for half-car models with two and four degrees of freedom. The presented results show that the control-design coupling can considerably improve the ride comfort in terms of reduced sprung mass pitch or heave acceleration with a relatively small sacrifice of vehicle handling and suspension stroke. The performance improvement is explained by the fact that the rear suspension controller uses state information from the front axle (and vice versa), which may be considered as a kind of preview action.

Keywords: Active suspension · Half-car model · Optimal control · Control coupling

1 Introduction

Half-car model introduces several effects which are not present in the basic quarter-car model, such as wheel-base filtering and sprung mass pitch dynamics. When designing an active suspension control system, decoupled controllers targeted to each axle are typically considered (see e.g. [1]). Such design relies on decoupling the half-car model into two separate quarter-car models based on satisfying specific mechanical- and control-design conditions, where the latter defines the ratio of pitch and heave acceleration penalization [2]. In this paper, it is investigated if further ride comfort improvement can be achieved through coupling the control actions of front and rear suspensions, i.e. by separating the tuning of heave and pitch acceleration penalizations.

The remaining part of the paper is organized in three sections. Section 2 contains details on the vehicle models and related controls, and introduces mechanical and control decoupling conditions. Section 3 details the methodology for evaluation of performance metrics based on standard deviations of system outputs (so-called

covariance analysis). The covariance analysis results are discussed in the same section, with emphasis on improvements obtained by front/rear axle control coupling. Concluding remarks are given in Sect. 4.

2   Active Suspension Modeling and Control

Two typical representations of half-car model are depicted in Fig. 1, and they include a two degree of freedom (DOF) model (Fig. 1a) and a four DOF model (Fig. 1b) [1]. The chosen state variables are front and rear suspension deflections and front and rear sprung mass velocities for the 2DOF model, and additional two state variables per axle corresponding to the tire deflections for the 4DOF model. The 2DOF model is described in the state-space form as [1]:

$$
\underbrace{\begin{bmatrix} \dot{z}_{sf} \\ \ddot{z}_f \\ \dot{z}_{sr} \\ \ddot{z}_r \end{bmatrix}}_{\dot{\mathbf{x}}} = \underbrace{\begin{bmatrix} 0 & 1 & 0 & 0 \\ 0 & 0 & 0 & 0 \\ 0 & 0 & 0 & 1 \\ 0 & 0 & 0 & 0 \end{bmatrix}}_{\mathbf{A}} \underbrace{\begin{bmatrix} z_{sf} \\ \dot{z}_f \\ z_{sr} \\ \dot{z}_r \end{bmatrix}}_{\mathbf{x}} + \underbrace{\begin{bmatrix} 0 & 0 \\ \frac{J_p + M_s l_f^2}{J_p M_s} & \frac{J_p - M_s l_f l_r}{J_p M_s} \\ 0 & 0 \\ \frac{J_p - M_s l_f l_r}{J_p M_s} & \frac{J_p + M_s l_r^2}{J_p M_s} \end{bmatrix}}_{\mathbf{B}} \underbrace{\begin{bmatrix} U_f \\ U_r \end{bmatrix}}_{\mathbf{u}} + \underbrace{\begin{bmatrix} -1 & 0 \\ 0 & 0 \\ 0 & -1 \\ 0 & 0 \end{bmatrix}}_{\mathbf{G}} \underbrace{\begin{bmatrix} w_f \\ w_r \end{bmatrix}}_{\mathbf{w}}, \quad (1)
$$

where $\mathbf{x}$ is the state vector, $\mathbf{A}$, $\mathbf{B}$, and $\mathbf{G}$ are the system, control input, and disturbance input matrices, respectively, $\mathbf{u}$ is the control input vector corresponding to front and rear active suspension actuator forces, and $\mathbf{w}$ is the ground velocity vector. The model parameters used throughout this paper are given at the end of Appendix.
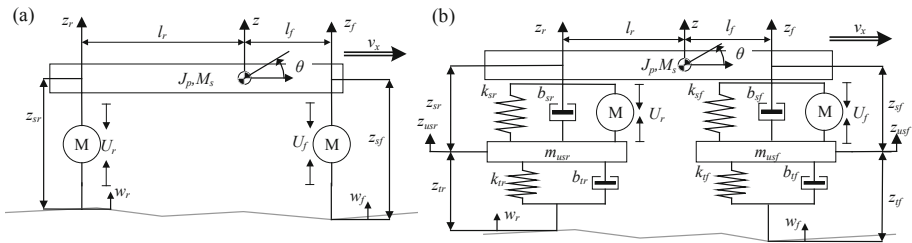
Fig. 1. Half-car model with two degrees-of-freedom (2DOF) (a) and four degrees of freedom (4DOF) (b)

Note that the matrix $\mathbf{B}$ contains two elements (b_{22} and b_{41}) which mechanically couple rear actuator force and front suspension dynamics, and vice versa, thus meaning that the control action at the rear axle affects front suspension states, and vice versa. In order to mechanically decouple front and rear suspension dynamics, these two terms have to be equal to zero, which gives the mechanical decoupling condition [1, 2]:

$$
J_p = M_s l_f l_r, \quad (2)
$$

where J_p is the pitch moment of inertia, M_s is the sprung mass, and l_f and l_r are distances between the center of gravity (CoG) and the front and rear axle, respectively (Fig. 1a).

The mechanical decoupling condition is rarely fully satisfied, but the ratio $J_p/(M_s l_f l_r)$ is close to 1 for most of vehicles. According to the vehicle data available in CarSim, this ratio is between 0.73 and 0.89 for all vehicle types considered therein. Thus, it is reasonable to assume that the mechanical decoupling condition is satisfied, which is confirmed by the analysis presented in Sect. 3 (along results presented in Fig. 2). Note that the decoupling condition (2) holds for the 4DOF model, as well [1, 2].

The active suspension is considered to be controlled by a linear quadratic regulator (LQR). The LQR-design cost function for 4DOF model includes penalization of root-mean-square (RMS) sprung mass heave $(\ddot{z})$ and pitch $(\ddot{\theta})$ accelerations, RMS front and rear tire deflections (z_{tf} and z_{tr}), and RMS front and rear suspension deflections (z_{sf} and z_{sr}) [1]:

$$J = \mathrm{E}\left(r_1 \ddot{z}^2 + r_2 \ddot{\theta}^2 + r_{3f} z_{tf}^2 + r_{3r} z_{tr}^2 + r_{4f} z_{sf}^2 + r_{4r} z_{sr}^2\right). \tag{3}$$

In the case of 2DOF model, the penalization terms corresponding to tire deflection are omitted: $r_{3f} = r_{3r} = 0$. Penalization coefficients of front and rear suspension deflection may be fixed (e.g. $r_{4f} = r_{4r} = 1$), while the ones related to front and rear tire deflections may be set to be proportional to those of corresponding suspension deflections (e.g. $r_{3f} = 10 \, r_{4f} = 10$). In this way we eliminate the solutions which do not result in practical designs, in a similar fashion as done in the quarter-car model [3] (see Appendix).

The cost function Eq. (3) can be rewritten into the LQ matrix form:

$$J = \mathrm{E}\left(\mathbf{x}^T \mathbf{Q} \mathbf{x} + \mathbf{u}^T \mathbf{R} \mathbf{u}\right), \tag{4}$$

where the state vector equals $\left[z_{sf}\, \dot{z}_f\, z_{sr}\, \dot{z}_r\right]^{\mathrm{T}}$ and $\left[z_{tf}\, \dot{z}_{usf}\, z_{sf}\, \dot{z}_f\, z_{tr}\, \dot{z}_{usr}\, z_{sr}\, \dot{z}_r\right]^{\mathrm{T}}$ for the 2DOF and 4DOF models, respectively, while the matrices $\mathbf{Q}$ (for 2DOF model) and $\mathbf{R}$ (for both models) read:

$$\mathbf{Q} = \begin{bmatrix} r_{4f} & 0 & 0 & 0 \\ 0 & 0 & 0 & 0 \\ 0 & 0 & r_{4r} & 0 \\ 0 & 0 & 0 & 0 \end{bmatrix}, \quad \mathbf{R} = \begin{bmatrix} \frac{r_1}{M_s^2} + r_2 \frac{l_f^2}{J_p^2} & \frac{r_1}{M_s^2} - r_2 \frac{l_f l_r}{J_p^2} \\ \frac{r_1}{M_s^2} - r_2 \frac{l_f l_r}{J_p^2} & \frac{r_1}{M_s^2} + r_2 \frac{l_r^2}{J_p^2} \end{bmatrix}. \tag{5}$$

The optimal state-feedback control law that minimizes the cost function Eq. (4) is defined for the 2DOF model as:

$$\left[U_{\mathrm{f}} \quad U_{\mathrm{r}} \right]^T = -\mathbf{K}\mathbf{x} = \begin{bmatrix} k_{11} & k_{12} & k_{13} & k_{14} \\ k_{21} & k_{22} & k_{23} & k_{24} \end{bmatrix} \left[z_{sf} \quad \dot{z}_f \quad z_{sr} \quad \dot{z}_r \right]^T, \tag{6}$$

The control decoupling condition follows from setting the cross-diagonal terms of control input penalization matrix $\mathbf{R}$ to zero, and it is given by [2]:

$$r_2 = \frac{J_p^2}{M_s^2 l_f l_r} r_1. \tag{7}$$

The same control decoupling condition is valid for 4DOF model, as well [1, 2]. Equation (7) when related to Eq. (3) implies the loss of a control degree of freedom, i.e. the pitch and heave criteria become coupled when the ratio r_2/r_1 is set to $J_p^2/(M_s^2 l_f l_r)$. Note that in case when the mechanical decoupling condition (2) is satisfied, the control design decoupling condition (7) reduces to $r_2 = l_f l_r r_1$.

3   Performance Analysis of Control-Design Coupling

Performance analysis of the considered active suspension control system is based on covariance analysis [4], which results in normalized RMS values of state variables with respect to zero-mean Gaussian white noise ground velocity **w**, which is a typical approximation of stochastic road profile [3]. Assuming that the active suspension closed-loop system is stable, standard deviations of state variables can be numerically obtained by solving variance equation, which is similar to Lyapunov equation [4]:

$$\mathbf{A}_{cl}\mathbf{X} + \mathbf{X}\mathbf{A}_{cl}^T + \mathbf{G}\mathbf{Q_w}\mathbf{G}^T = 0, \tag{8}$$

where $\mathbf{A}_{cl}$ is the closed-loop system matrix $\mathbf{A}_{cl} = \mathbf{A} - \mathbf{B}\mathbf{K}$, $\mathbf{X}$ is the state covariance matrix, and $\mathbf{Q_w}$ is the power spectral density matrix of ground velocity. The term $\mathbf{G}\mathbf{Q_w}\mathbf{G}^T$ should take into account the time delay between front and rear ground velocity inputs because of introduced control coupling. This is an extension of the decoupled control approach considered in [1], where the time delay is not taken into account. For the considered 2D case, the ground velocity input is represented by [5]:

$$\mathbf{w} = \begin{bmatrix} w_f \\ w_r \end{bmatrix} = \begin{bmatrix} w(t) \\ w(t - t_{wb}) \end{bmatrix} \tag{9}$$

where $t_{wb} = (l_f + l_r)/v_x$ is time delay between axles, with v_x denoting the vehicle longitudinal velocity. Such white noise input is represented by its power spectral density matrix [5, Chap. 29]:

$$\mathbf{Q_w} = \frac{2}{\pi}\int\limits_0^\infty R_\mathbf{w}(\tau)\cos(\Omega)\tau d\tau = \frac{2}{\pi}\int\limits_0^\infty q_w \begin{bmatrix} \delta(\tau) & \delta(\tau + t_{wb}) \\ \delta(\tau - t_{wb}) & \delta(\tau) \end{bmatrix} \cos(\Omega)\tau d\tau \tag{10}$$

where δ is Dirac function. $\mathbf{Q_w}$ is now 2×2 matrix with power spectral densities of ground velocities. If we partition the matrix $\mathbf{G}$ from Eq. (1) such that $\mathbf{G} = \begin{bmatrix} \mathbf{G}_1^{4\times1} & \mathbf{G}_2^{4\times1} \end{bmatrix}$, i.e. such that each axle has its own input matrix, and insert it into $\mathbf{G}\mathbf{Q_w}\mathbf{G}^T$ of Eq. (8), while taking into account Eq. (10) we get [5, chap. 29]:

$$\mathbf{Q}_{wn} = \mathbf{G}\mathbf{Q_w}\mathbf{G}^T = q_w \left[\mathbf{G_1}\mathbf{G}_1^T + \mathbf{G_2}\mathbf{G}_2^T + e^{\mathbf{A}t_{wb}}\mathbf{G_1}\mathbf{G}_2^T + \mathbf{G_2}\mathbf{G}_1^T e^{\mathbf{A}^T t_{wb}} \right], \qquad (11)$$

where $e^{\mathbf{A}t_{wb}}$ is matrix exponential of $\mathbf{A}t_{wb}$. If we set $q_w = 2\pi AV$, where A is the road roughness coefficient [1], insert $\mathbf{Q}_{wn}$ given by Eq. (11) into Eq. (8), and divide the obtained results with square root of q_w we get normalized RMS values of state variables. The normalized RMS values of output variables can be obtained from $\mathbf{Y} = \mathbf{C}_{cl}\mathbf{X}\mathbf{C}_{cl}^T$, where $\mathbf{C}_{cl} = \mathbf{C} - \mathbf{DK}$ is the closed-loop output matrix, and $\mathbf{C}$ and $\mathbf{D}$ are the matrices of model output equation ($\mathbf{y} = \mathbf{Cx} + \mathbf{Du}$). The reason for why the covariance equation cannot be normalized before being solved lies in Eq. (11), where v_x is implicitly present through $t_{wb} = (l_f + l_r)/v_x$.

Figure 2 shows the performance plot of 2DOF model, obtained by varying the mechanical decoupling ratio $J_p/(M_s l_f l_r)$ between 0.5 and 1.5, with the control-design decoupling condition (7) satisfied, i.e. $r_2 = r_1 J_p^2/(M_s^2 l_f l_r)$ held, and suspension stroke penalization coefficients in Eq. (3) set to $r_{4f} = 1$ and $r_{4r} = l_f/l_r$ (it can be readily shown that this particular choice of ratio r_{4f}/r_{4r} ensures same front and rear suspension strokes), and varying penalization of heave acceleration r_1. It can be observed from the plot that by increasing the pitch inertia J_p (higher mechanical coupling ratio), the RMS heave acceleration is somewhat increased while the RMS pitch acceleration (shown in color) is somewhat decreased for the same value of suspension stroke. This trend is more pronounced for the case of lower heave acceleration penalization coefficient r_1.
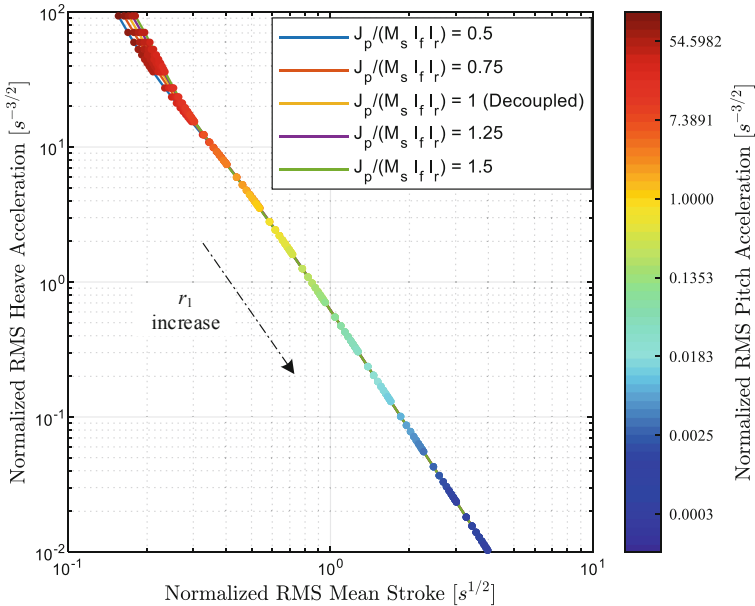
Fig. 2. Performance plot of 2DOF model for varying mechanical coupling ratio and heave penalization (r_1), with fixed suspension stroke penalization ($r_{4f} = 1$ and $r_{4r} = l_f/l_r$) and satisfied control decoupling condition ($r_2 = r_1 J_p^2/(M_s^2 l_f l_r)$).

Note that the front and rear suspension strokes are condensed in Fig. 2 into the mean suspension stroke, in order to present the results in a compact manner, with no loss of generality since the front and rear suspension stroke are equally penalized.

If the system is mechanically decoupled ($J_p/(M_s l_f l_r) = 1$), the front suspension actuator force will not affect the rear suspension states, and vice versa. If along with the mechanical decoupling condition, the control decoupling condition is satisfied, i.e. $r_2/r_1 = l_f l_r$ (1.875 for the particular vehicle data listed in Appendix), the state controller gain matrix $\mathbf{K}$ and the matrix $\mathbf{R}$ are equal to:

$$\mathbf{K} = \begin{bmatrix} 812.4 & 987.3625 & 0 & 0 \\ 0 & 0 & 677 & 822.8 \end{bmatrix}, \quad \mathbf{R} = 10^{-5} \cdot \begin{bmatrix} 0.1515 & 0 \\ 0 & 0.1818 \end{bmatrix}$$

This means that the front actuator (U_f) does not use rear suspension states ($z_{sr} \dot{z}_r$), as feedback gains corresponding to the rear suspension states, i.e. cross-coupling gains, are equal to zero. The same conclusion holds for rear actuator and front suspension states.

The control coupling is reflected in appearance of non-zero cross-coupling terms in the state controller gain matrix $\mathbf{K}$, where there are two characteristic cases. The first case is defined by the inequality $r_2/r_1 > l_f l_r$, which results in the following matrices $\mathbf{K}$ and $\mathbf{R}$ (given for $r_2/r_1 = 10$):

$$\mathbf{K} = \begin{bmatrix} 559.9 & 790.94 & 252.5 & 196.42 \\ 252.5 & 196.42 & 424.5 & 626.38 \end{bmatrix}, \quad \mathbf{R} = 10^{-4} \cdot \begin{bmatrix} 0.0771 & -0.0744 \\ -0.0744 & 0.1074 \end{bmatrix}$$

The second case, in which the ratio $r_2/r_1 < l_f l_r$, here $r_2/r_1 = 0.1$, results in:

$$\mathbf{K} = 10^3 \cdot \begin{bmatrix} 1.6109 & 1.3367 & -0.7985 & -0.3493 \\ -0.7985 & -0.3493 & 1.4755 & 1.1721 \end{bmatrix},$$
$$\mathbf{R} = 10^{-6} \cdot \begin{bmatrix} 0.8953 & 0.7438 \\ 0.7438 & 0.9256 \end{bmatrix}$$

The above LQR parameter results for the two characteristic cases point out that positive cross-diagonal elements of matrix $\mathbf{R}$ cause negative LQR cross-gains (elements k_{13}, k_{14} and k_{21}, k_{22}), and negative cross-diagonal elements of matrix $\mathbf{R}$ cause positive LQR cross-gains. In both cases this means that, even for mechanically decoupled suspension model, the rear suspension controller gets information from front axle, which could be viewed as some sort of preview. Also, in the case when cross-gains are positive, front and rear suspension forces will be in the same direction with respect to same state variable, thus attempting to reduce pitch motion (note that in this case $r_2 > r_1$ holds), but from this we cannot determine at what cost.

Figure 3 shows the obtained performance plot of 2DOF model from Fig. 1a, which indicates the trade-off between ride comfort and suspension stroke. For the case of control-design decoupling (i.e. when the condition (7) is satisfied), the pitch acceleration has the same trend as heave acceleration (see dark orange line in Fig. 3 and cf. the

results from Fig. 2 for the decoupled case), and it decreases as the suspension stroke increases. Thus, there are two conflicting criteria: heave/pitch acceleration and suspension stroke.

In the control-design coupling case, the weighting factors r_1 and r_2 can be set independently, thus resulting in one control degree-of-freedom more and 3D performance plot in Fig. 3 (the three performance criteria become conflicting to each other), compared to the control decoupling case represented by 2D plot. One may increase r_2 while keeping r_1 constant to come below the decoupled-case performance line, i.e. to reduce pitch acceleration without significantly affecting heave acceleration and suspension strokes. More specifically, when considering point E_c in comparison with the decoupled-case point E, the RMS pitch acceleration is reduced by 86% with no change in RMS heave acceleration and with RMS mean suspension stroke increase of 1% (note that front suspension stroke is increased by 4% and rear suspension stroke decreased by 3%). It should be noted that while the pitch acceleration can be reduced without significant increase of suspension strokes, the heave acceleration cannot be reduced without affecting the suspension stroke.
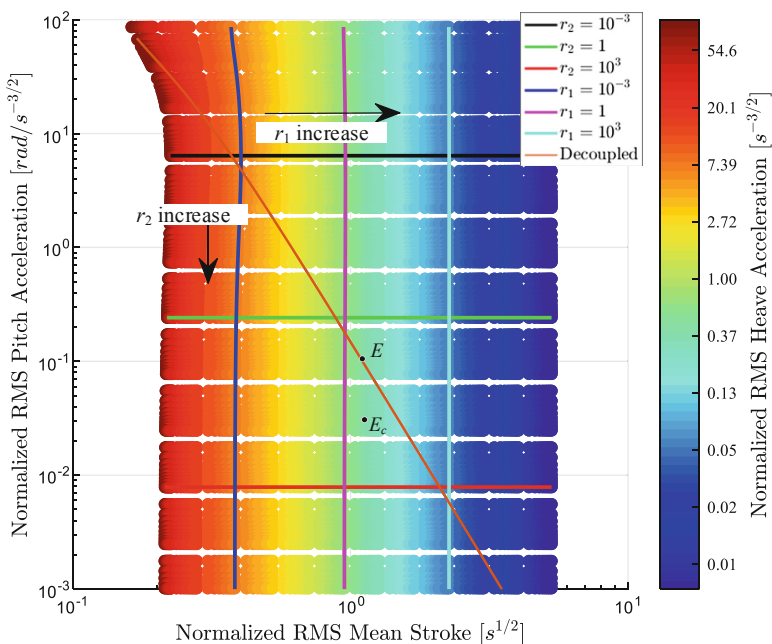
Fig. 3. Performance plot for control design coupling case of mechanically decoupled 2DOF model $\left(J_p/(M_s l_f l_r) = 1 \right)$, obtained for fixed suspension stroke penalizations $\left(r_{4f} = 1, r_{4r} = l_f/l_r \right)$ and varying heave (r_1) and pitch (r_2) penalizations.

Figure 4 shows the trade-off between ride comfort, vehicle handling and suspension stroke for the 4DOF model. Here, the ratio of tire deflection and suspension stroke

penalizations is set to $r_3/r_4 = 10$, as this results in a good trade-off between tire deflection and suspension stroke (see [3] and Appendix), and both front and rear states are equally penalized ($r_{3f} = r_{3r} = r_3$, $r_{4f} = r_{4r} = r_4 = 1$). The front and rear RMS tire deflections and RMS suspension deflections are represented by their mean values, similarly as in the case of 2DOF model. The control decoupling case (magenta line; $r_2/r_1 = l_f l_r$) results in qualitatively similar trade-off between heave/pitch acceleration and suspension stroke as observed in the 2DOF model case (cf. Figure 3 and note that the RMS values of suspension and tire deflection are related to each other for fixed ratio r_3/r_4 selected).
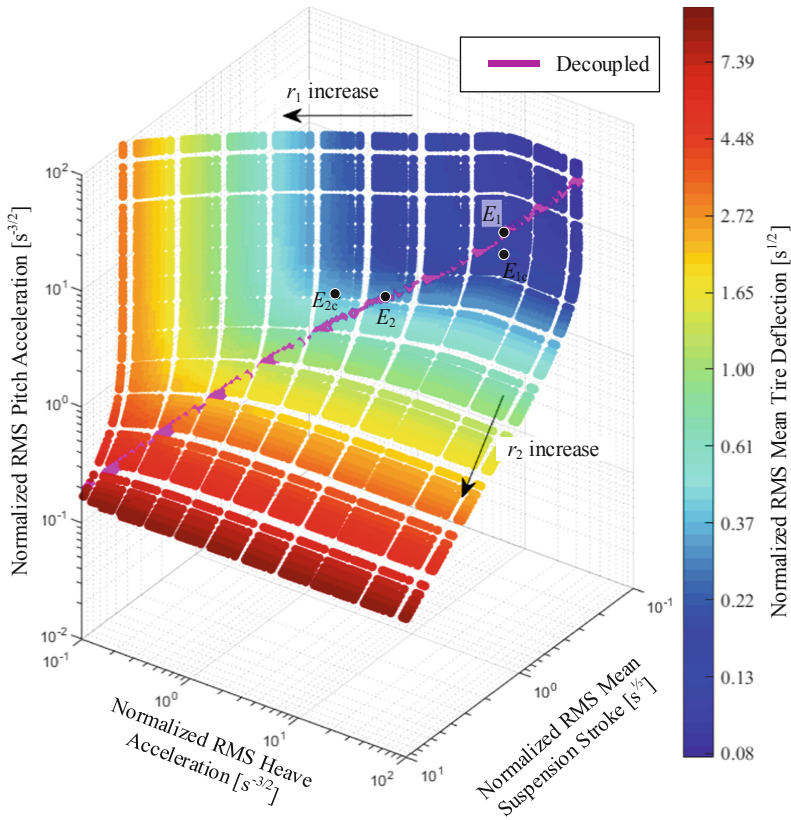
Fig. 4. Performance plot for control-design coupling case of mechanically decoupled 4DOF model ($J_p/(M_s l_f l_r) = 1$), obtained for fixed tire deflection penalizations $\left(r_{3f} = r_{3r} = 10\right)$ and fixed suspension deflection penalization ($r_{4f} = r_{4r} = 1$), and varying heave (r_1) and pitch (r_2) penalization.

However, when control-design coupling is exploited $(r_2/r_1 \neq l_f l_r)$, pitch acceleration or heave acceleration can be additionally decreased with mostly minor sacrifices in tire deflection and/or suspension stroke (generally, there are four conflicting criteria, i.e. three in the particular case of fixed ratio r_3/r_4). For instance, when considering points E_1 and E_{1c} in Fig. 4, the RMS pitch acceleration is reduced by 26% at the cost of RMS mean suspension stroke increase of 2% and RMS mean tire deflection increase of 6%, without impact on heave acceleration.

Furthermore, when considering points E_2 and E_{2c} in Fig. 4, the RMS heave acceleration can be reduced by 21% with unchanged level of RMS pitch acceleration, and with only 3% increase in RMS mean tire deflection and less than 9% increase in RMS mean suspension stroke. The control coupling benefits are generally lower than for the 2DOF model, as a consequence of introduction of unsprung mass dynamics and tire deflection criteria.

4   Conclusion

The benchmark performance of half-car model equipped with LQR-controlled active suspension, expressed in terms of trade-off of normalized RMS heave and pitch accelerations, tire deflections and suspension strokes, has been evaluated in the cases of front/rear axle mechanical coupling and control-design coupling. The control-design coupling, in which the heave and pitch accelerations penalizations can be set separately, results in improvements of ride comfort without significant deterioration of handling and suspension stroke criteria when compared to the decoupled case. Unlike in the decoupled case, the rear-axle suspension controller acts on the front-axle state measurements (and vice versa), thus providing a kind of preview action that improves the performance. However, from the implementation point of view, exploiting front/rear axle control coupling may result in more complex design of realistic control system (including observers) and eventually less robust behavior when compared to decoupled, quarter car model-based controllers.

Apart from designing and analyzing more realistic control system, the future work can be directed to expanding the knowledge gained from the presented analysis on a full-car model, which has additional degree of freedom related to roll dynamics, and/or on the case of added road preview control. Furthermore, adaptive control schemes could be derived, which would, for instance, emphasize either heave suppression or pitch suppression depending on the driving conditions or driver's preferences.

Appendix

Applying the covariance analysis to the quarter-car model (a half of the model shown in Fig. 1b) and the cost function (cf. Eq. (3)):

$$J = \mathrm{E}\left(r_0\ddot{z}^2 + r_1 z_t^2 + r_2 z_s^2\right), \tag{12}$$

gives the performance plot shown in Fig. 5, which indicates the trade-off between the three conflicting criteria in a similar (but more illustrative way) than the carpet plots given in [1]. Although the three criteria are conflicting, it can be observed from the plot in Fig. 5 that there exists an area bounded roughly by lines corresponding to $r_1 = 0.01$ and $(r_1/r_2)_{max} = 1000$ in which both RMS tire deflection and RMS suspension deflection monotonically fall with increasing sprung mass acceleration. Thus, this practical design area can be associated with tire deflection penalization (r_1) being stronger than suspension deflection penalization (r_2). Satisfying trade-off between RMS tire deflection and suspension deflection is obtained for $r_1/r_2 = 10$ (cf. intersections between equally colored solid and dashed lines in Fig. 5), which is used as design setting related to 4DOF model in the main body of this paper ($r_3/r_4 = 10$, therein).
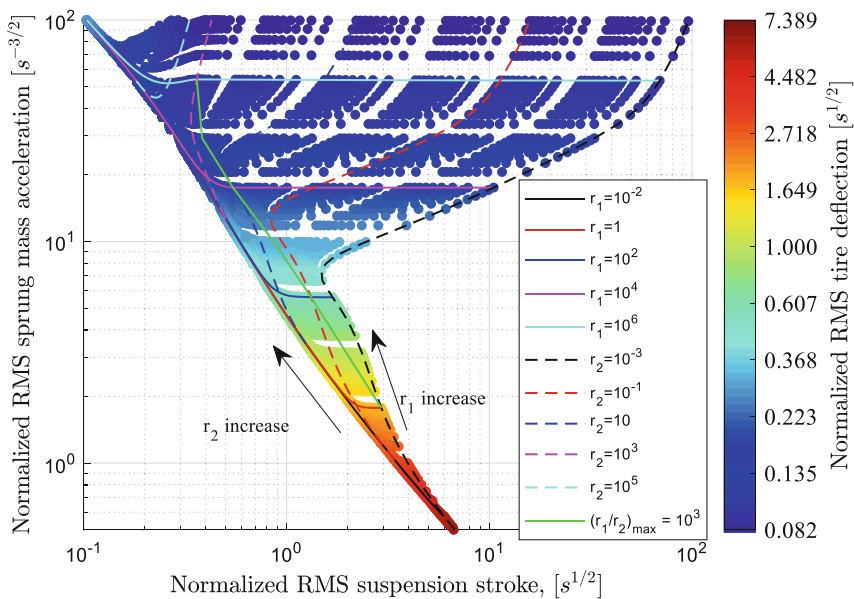
Fig. 5. Performance plot of quarter-car model obtained with sprung mass penalization r_0 set to 1, and varying tire deflection penalization (r_1) and suspension stroke penalization (r_2).

The half-car model parameters used in the main body of this paper are [1]: $J_p = 2475$ kgm^2, $M_s = 1100$ kg, $l_f = 1.25$ m, $l_r = 1.75$ m, $m_{usf} = m_{usr} = 40$ kg, $k_{tf} = k_{tr} = 160000$ N/m, $b_{tf} = b_{tr} = 0$ Ns/m. The quarter-car model parameters used to obtain the plot in Fig. 5 are [3]: $m_s = 400$ kg, $m_{us} = 40$ kg, $k_t = 160000$ N/m, $b_t = 0$ Ns/m.

References

1. Hrovat, D.: Optimal suspension performance for 2-D vehicle models. J. Sound Vib. **146**(1), 93–110 (1991)
2. Krtolica, R., Hrovat, D.: Optimal active suspension control based on a half-car model: an analytical solution. IEEE Trans. Autom. Control **37**(4), 528–532 (1992)
3. Hrovat, D.: Survey of advanced suspension developments and related optimal control applications. Automatica **33**(10), 1781–1817 (1997)
4. Moore, J.B., Anderson, B.: Optimal Control – Linear Quadratic Methods. Prentice-Hall Inc., USA (1989)
5. Mastinu, G., Ploechl, M.: Road and Off-Road Vehicle System Dynamics Handbook. CRC Press, Boca Raton (2014)